

Supporting Information: Improved Parametrization of Lithium, Sodium, Potassium, and Magnesium ions for All-Atom Molecular Dynamics Simulations of Nucleic Acid Systems.

Jejoong Yoo[†] and Aleksei Aksimentiev^{*,†,‡}

*Department of Physics, University of Illinois at Urbana–Champaign, 1110 West Green Street,
Urbana, Illinois 61801, and Beckman Institute for Advanced Science and Technology*

E-mail: aksiment@illinois.edu

*To whom correspondence should be addressed

[†]Department of Physics

[‡]Beckman Institute for Advanced Science and Technology

Osmotic pressure of bulk electrolytes

General MD methods

All MD simulations were carried out in a constant-temperature/constant-area ensemble using the Gromacs 4.5.1 package¹ and a 2 fs integration time step. The temperature was controlled using the Nosé-Hoover scheme.^{2,3} In all simulations except of DMP⁻ solutions, the temperature was set to 298 K. The simulations of DMP⁻ solutions were done at $T = 308$ K to match the conditions of the corresponding osmotic pressure measurements.⁴ The normal pressure was kept constant at 1 bar using the Parrinello-Rahman scheme.⁵ We used 7-to-8 Å switching scheme to evaluate van der Waals forces and particle-Mesh Ewald (PME) summation⁶ to evaluate long-range electrostatic forces. Our PME scheme employed a 1.2-Å Fourier-space grid spacing and a 12 Å cutoff for the real-space Coulomb interaction. SETTLE⁷ and LINCS⁸ algorithms were used to constrain covalent bonds to hydrogen in water, and in Ac⁻, DMP⁻ and DNA, respectively.

Force fields

In this work, we considered the following three sets of force field parameters. The first one was the standard parameter set distributed with the CHARMM27 force field,⁹ which included ion parameters for Na⁺, K⁺, Mg²⁺, and Cl⁻ developed by Beglov and Roux.¹⁰ The second set combined the standard AMBER99 parameters¹¹ for biomolecules with Li⁺, Na⁺, K⁺, and Cl⁻ ion parameters recently developed by Joung and Cheatham¹² and Mg²⁺ ion parameter of the CHARMM27 force field. We deliberately chose the Joung and Cheatham parametrization of ions over the Åqvist parametrization¹³ as the latter was reported to cause spontaneous crystallization of NaCl and KCl solutions below the experimental solubility limit.¹² The third set combined the CHARMM27 parameters for biomolecules with the Joung and Cheatham parameters for Li⁺, Na⁺, K⁺, and Cl⁻ ions. As the standard CHARMM force field lacks parameters for Li⁺, the last combination is of particular value for systematic studies of the influence of electrolyte type on the structure and dynamics of biomolecules.

The standard Lennard-Jones (LJ) parameters (σ and ϵ) for a pair of atoms were determined using the Lorentz-Berthelot mixing rule, which is the standard method for both CHARMM and AMBER force fields. The TIP3P model of water¹⁴ was used with all three sets of parameters. Corrections to the LJ σ parameter of a specific cation-anion pair were introduced using the non-bond_params entry in the Gromacs topology files. Following the language used in the previous study,¹⁵ we refer to such adjustments NBFIX corrections. Our results for the first two sets of parameters (standard CHARMM and AMBER) are summarized in Table 1 in the main text, and the results for the CHARMM-Cheatham combination are summarized in Table S1.

Table S1: NBFIX corrections for cation-acetate/phosphate terminal oxygen pairs for a combination of Joung and Cheatham parameters for cations and the CHARMM27 parameters for acetate and phosphates. Each entry specifies the difference ($\Delta\sigma$, expressed in Å) between the NBFIX value of LJ σ that reproduces the experimental osmotic pressure data and the standard LJ σ value computed using the Lorentz-Berthelot mixing rule.

	O–Ac [−] / DMP [−]
Li ⁺	0.180
Na ⁺	0.090
K ⁺	0.170

Setup of osmotic pressure simulations

Our calculations of the osmotic pressure of bulk electrolytes follow the method described by Luo and Roux.¹⁵ Each simulation system contained two compartments separated by two virtual semipermeable membranes aligned with the xy plane. One compartment contained an electrolyte solution while the other contained pure water. While water could freely pass through the membranes separating the two compartments, the ions were subject to the force of half-harmonic planar potentials whose action mimicked the ideal behaviors of a semipermeable membrane that induces

osmosis. Specifically, we used the following expression for the confining force:

$$F_i^{\text{memb}} = \begin{cases} -k(z_i - D/2) & \text{for } z_i > D/2 \\ 0 & \text{for } |z_i| \leq D/2 \\ -k(z_i + D/2) & \text{for } z_i < -D/2 \end{cases} \quad (1)$$

where z_i is the z coordinate of ion i , D is the width of the electrolyte compartment, and the force constant $k = 4000$ kJ/mol·nm. Such half-harmonic potentials are implemented in the MDRUN program of Gromacs 4.5.1 package.¹ The total instantaneous force applied to both membranes by the ions, which is equal and opposite to the force applied to the ions by the membrane, $\sum_i F_i^{\text{memb}}$, was recorded every 2 fs. The instantaneous osmotic pressure was obtained by dividing the instantaneous total force on the membranes by the total area of the membranes. Each simulation ran until the osmotic pressure reached a constant value, which was determined using the following procedure.¹⁶ As recommended by Schiferl and Wallace, the entire MD trajectory was split into 24 blocks. The simulation was terminated if the block-average values passed the following four statistical tests:¹⁶ Mann-Kendall test for lack of trend in block averages, Mann-Kendall test for lack of trend in variance of block averages, W test for normality of block averages, and von Neumann test for serial correlation of block averages.

Following the convention used in experimental measurements of osmotic pressure, the molal concentration of an electrolyte solution, m , is calculated using mean mass densities: $m = (\bar{\rho}^{\text{salt}}/M^{\text{salt}})/\bar{\rho}^{\text{water}}$, where M^{salt} is the molar mass of the salt, $\bar{\rho}^{\text{salt}} = \bar{\rho}^{\text{cation}} + \bar{\rho}^{\text{anion}}$ and $\bar{\rho}^{\text{water}}$ are the mean mass densities of the ions and water, respectively. In our analysis of the simulation trajectories, the mean mass density was calculated by averaging over the volume defined by $|z| < 1.5$ nm (See Figure 2C). To estimate statistical error of the molal concentration, the entire MD trajectory was split into 10-ns blocks, and the standard deviation of block-wise molal concentrations was calculated.

In our search for parameters that reproduce the experimental osmotic pressure data, we simulated electrolyte solutions at four concentrations for each cation-anion pair. Table S2 lists the

compartments' geometry and the ion composition in each simulation. For each type of electrolyte solution, we ran a series of osmotic pressure simulations starting from the solution of the highest concentration (~ 3 m) and the standard value of LJ σ ($\Delta\sigma = 0$). Next, we gradually increased the value of LJ σ until the simulated osmotic pressure matched the experimental one. Figures S1-S3 show the results of the parameterization simulations. The final values of the NBFIX corrections, $\Delta\sigma$, are given in Table 1 and S1. To verify our results, each system was simulated at three lower concentrations with and without the NBFIX corrections.

Calculation of the osmotic coefficient ϕ

Osmotic pressure of an ideal electrolyte solution, π^{id} , is proportional to molal concentration of electrolyte (m):

$$\pi^{\text{id}}(m) = \frac{RT\nu}{\bar{V}}m, \quad (2)$$

where R is the gas constant, T is temperature in Kelvin, \bar{V} is the molar volume of pure water at 1 bar and room temperature, and ν is the total number of cations and anions per formula unit ($\nu = 2$ and 3 for 1-1 and 1-2 electrolyte solutions, respectively).¹⁷ At a given molal concentration m , the osmotic coefficient $\phi(m)$ is obtained by dividing the computed osmotic pressure p by the ideal osmotic pressure: $\phi = p/\pi^{\text{id}}$.

Parametrization of magnesium-hexahydrate ($\text{Mg}(\text{H}_2\text{O})_6^{2+}$)

As the lifetime of a water molecule within the first solvation shell of Mg^{2+} is $\sim 10 \mu\text{s}$,¹⁸ we assumed in this study that the $\text{Mg}(\text{H}_2\text{O})_6^{2+}$ complex would stay intact over the time scale of our MD simulations. To distinguish water molecules of the first solvation shell of Mg^{2+} from bulk water and thereby enable application of NBFIX corrections to the oxygens of the first solvation shell water, we treated each Mg^{2+} ion and the six surrounding water molecules as a $\text{Mg}(\text{H}_2\text{O})_6^{2+}$ complex. A sample topology of $\text{Mg}(\text{H}_2\text{O})_6^{2+}$ is included in the Supporting Information file `sample_gromacs_charmm.top` (see below). The parameters for Mg^{2+} and water in the complex were

taken from the CHARMM27 force field⁹ and the TIP3P water model,¹⁴ respectively. Partial charges of the TIP3P water in the complex were adjusted to increase the dipole moment of TIP3P water by 1 debye, as suggested by a recent study using the AMOEBA polarizable force field.¹⁹

Although the $\text{Mg}(\text{H}_2\text{O})_6^{2+}$ structure was very stable in our test MD simulations, all production simulations utilized an additional restraining potential between Mg^{2+} and water oxygens, which ensured that all six water molecules in the complex remained in proximity of Mg^{2+} . Specifically, we used a half-harmonic potential that turns on at a separation of 2.5 Å, which is ~ 0.5 Å longer than the equilibrium Mg–O distance, Figure S4B. The force constant of each restraint was 500,000 kJ/mol·nm. The effects of such restraining potential on the outcome of our simulations was negligible, as the restraints neither altered the equilibrium Mg–O distance nor the vibration dynamics of water.

We have also tested another $\text{Mg}(\text{H}_2\text{O})_6^{2+}$ topology, in which Mg^{2+} and water oxygen distances were constrained to 1.94 Å using LINCS.⁸ In the latter case (which we refer to as rigid $\text{Mg}(\text{H}_2\text{O})_6^{2+}$), the bonds between Mg^{2+} and water oxygen were not taken into account in the calculations of non-bond exclusions. Figure S4C and D plot the osmotic coefficients simulated using the two models of $\text{Mg}(\text{H}_2\text{O})_6^{2+}$. The results are in good agreements, which indicates that the rigid model of $\text{Mg}(\text{H}_2\text{O})_6^{2+}$ can be used with packages that do not support half-harmonic restraints.

Simulations of the DNA array

Setup of simulations

An array of 64 double-stranded DNA molecules was built by replicating a pre-equilibrated simulation box that contained a single DNA duplex, poly(dG₂₀)·poly(dC₂₀), in solution. Initially, 64 copies of the DNA duplex were placed inside a cylinder 11 nm in radius, and water and ions outside the cylinder were deleted. The distance between the two neighboring duplexes was ~ 26 Å. Under the periodic boundary conditions, the DNA molecules were effectively infinite and aligned parallel to one another along the z axis. Water was added around this 11 nm-radius DNA bundle, increasing

the size of the simulation system to $\sim 29 \times 29 \times 6.8 \text{ nm}^3$ and $\sim 580,000$ atoms. In this work, we report data for two DNA array systems different by their ion composition. In the first system (system I), random replacement of water molecules with 2980 Na^+ and 420 Cl^- ions produced a 250 mM concentration of NaCl in the volume outside the DNA array after 20-ns equilibration. The second system (system II) was produced by randomly replacing water molecules of the original system with 750 Mg^{2+} , 1480 Na^+ , and 420 Cl^- ions. In the second system, the ion concentration outside the DNA array was 25 mM MgCl_2 and 250 mM NaCl.

All simulations of the DNA array were carried out in the presence of a harmonic potential that applied restraining forces to the phosphorus atoms of the DNA molecules, confining the latter to a cylindrical volume. The harmonic potential was defined as

$$V^{\text{wall}}(r) = \begin{cases} \frac{1}{2}k(r - R_0)^2 & \text{for } r > R_0, \\ 0 & \text{for } r \leq R_0, \end{cases} \quad (3)$$

where r is distance from the phosphorus atom to the center of the DNA array, R_0 is the radius of the confining cylinder (12 and 11 nm for system I and II, respectively), and k it the force constant (100 kJ/mol·nm). In such a setup, the internal pressure of the DNA array is equal to the pressure exerted by this half-harmonic wall on the DNA. Ions and water were not subject of the above potential. To determine the influence of the NBFIX corrections on the properties of the DNA array, each system was simulated for ~ 70 -ns with and without the NBFIX corrections. These simulations employed the CHARMM force field. All other simulations protocols were the same as in our simulations of the osmotic pressure of bulk electrolytes.

Analysis procedures

The snapshots of representative DNA conformations were made using the last 2 ns of the corresponding 70 ns production trajectory. Approximate location of each DNA helix was determined by averaging x, y coordinates of the helix's center of mass. The local density of cations within the xy plane was calculated by averaging the number of cations using square $\sim 2\text{\AA} \times 2\text{\AA}$ bins.

To make the histograms of the DNA-DNA distances, the coordinates of the center of mass of each DNA duplex were recorded every 2 ps for the last 15 ns of the corresponding production run. Then, the projection of the DNA-DNA distance onto the xy plane was calculated for all DNA pairs in all frames. Next, histograms of the distance data were made using a 0.02\AA bin width. Finally, the counts in all bins of the histograms were divided by the number of the frames used in the analysis.

Sample Gromacs topology files

The following sample Gromacs topology files with our sets of NBFIX corrections are available:

sample_gromacs_charmm.top contains a sample topology file for the CHARMM27 force field with our NBFIX corrections.

sample_gromacs_amber.top contains a sample topology file for the AMBER force field with our NBFIX corrections

sample_gromacs_charmm_cheatham.top contains a sample topology file for the CHARMM27 force field in combination with the Joung and Cheatham ion parameters.

Table S2: Geometry and concentration of the systems used in the simulations of the osmotic pressure of bulk electrolytes.

Cation	Anion	Compartment vol. ^a	Numbers			Conc. ^b
			Cation	Anion	Water	
Li ⁺ , Na ⁺ , or K ⁺	Ac ⁻ or DMP ⁻	5 × 5 × 5 (5 × 5 × ~ 3.5)	20	20	~ 6,000	~ 0.3
			50	50	~ 6,000	~ 0.7
			100	100	~ 6,000	~ 1.4
			200	200	~ 6,000	~ 2.8
Li ⁺ , Na ⁺ , or K ⁺	Cl ⁻	6 × 6 × 4 (6 × 6 × ~ 4)	50	50	~ 9,500	~ 0.3
			100	100	~ 9,500	~ 1.2
			200	200	~ 9,500	~ 2.4
			300	300	~ 9,500	~ 3.5
Mg ²⁺	Ac ⁻	5 × 5 × 5 (5 × 5 × ~ 3)	20	40	~ 5,000	~ 0.3
			50	100	~ 5,000	~ 0.7
			100	200	~ 5,000	~ 1.4
			200	400	~ 5,000	~ 2.9
Mg ²⁺	Cl ⁻	6 × 6 × 6 (6 × 6 × ~ 2.5)	50	100	~ 7,500	~ 0.5
			100	200	~ 7,500	~ 0.8
			200	400	~ 7,500	~ 1.6
			300	600	~ 7,500	~ 2.3

^a Volumes of the electrolyte solution and the pure water (in parenthesis) compartments in nm³.

^b Approximate molal concentration in the electrolyte solution compartment.

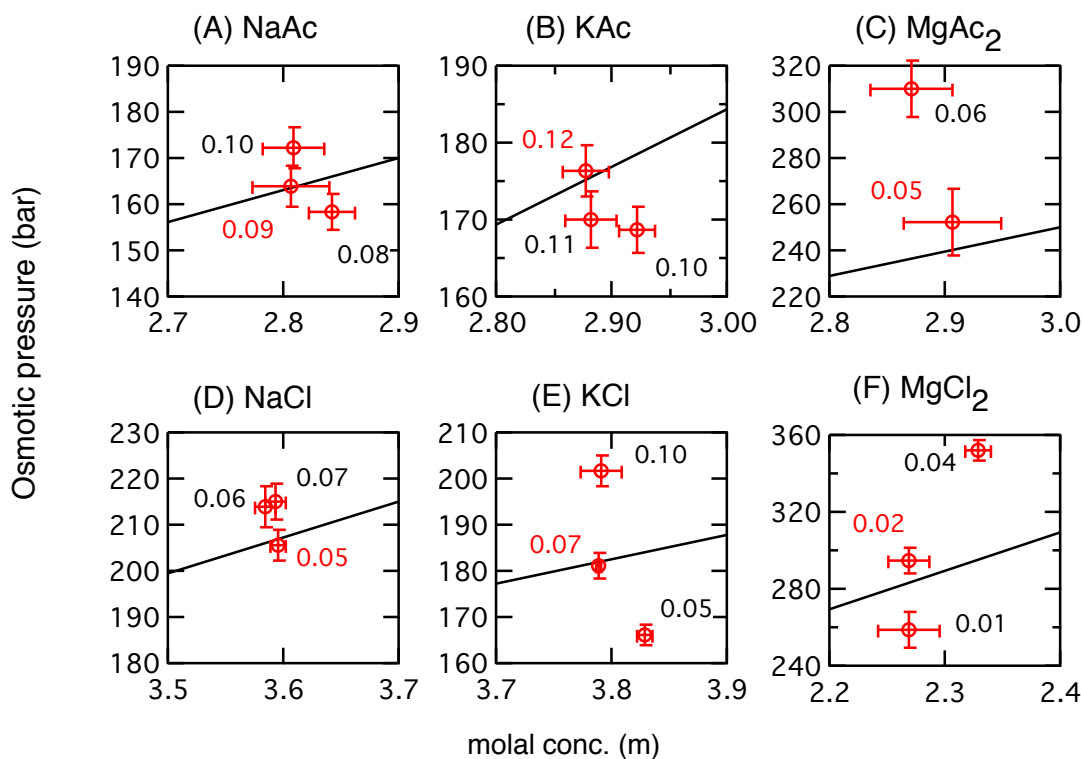


Figure S1: The effect of NBFIX corrections on the osmotic pressure of Na-Ac (A), K-Ac (B), Mg-Ac (C), Na-Cl (D), K-Cl (E), and Mg-Cl (F) electrolyte solutions. All simulations reported in this figure used the standard CHARMM27 force field and NBFIX correction $\Delta\sigma$ to the standard LJ σ parameter of the corresponding ion pair. Red circles plot the simulated osmotic pressure for the indicated values of the $\Delta\sigma$ correction (Å). Black lines show the experimental osmotic pressure values. Values of $\Delta\sigma$ that reproduce the experimental osmotic pressure are highlighted in red and are summarized in Table 1.

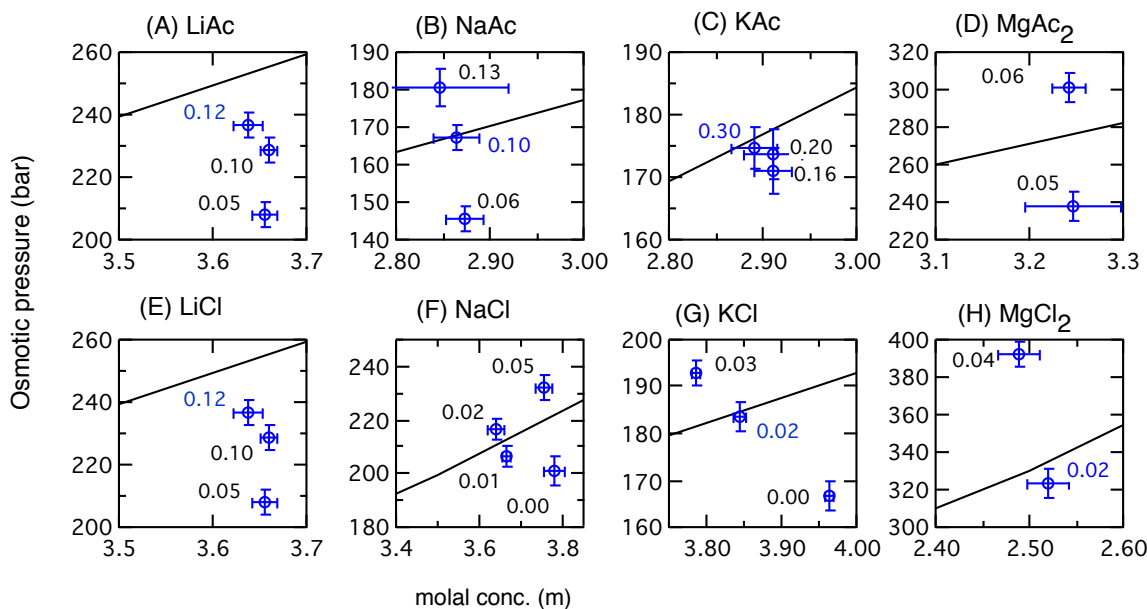


Figure S2: The effect of NBFIX correction on the osmotic pressure of Li-Ac (A), Na-Ac (B), K-Ac (C), Mg-Ac (D), Li-Cl (E), Na-Cl (F), K-Cl (G), and Mg-Cl (H) electrolyte solutions. All simulations reported in this figure used the standard AMBER parameter set for Ac^- , Joung and Cheatham parameters for monovalent ions,¹² Mg^{2+} of the CHARMM27 force field and NBFIX correction $\Delta\sigma$ to the standard LJ σ parameter of the corresponding ion pair. Blue circles plot the simulated osmotic pressure for the indicated values of the $\Delta\sigma$ correction (Å). Black lines show the experimental osmotic pressure values. Values of $\Delta\sigma$ that reproduce the experimental osmotic pressure are highlighted in blue and are summarized in Table 1. In the case of data shown in panels (D) and (F), the final $\Delta\sigma$ values were chosen to be 0.055 and 0.015, respectively, by interpolation. For LiCl (E), the value of 0.12 was chosen because corrections greater than 0.12 did not change the simulated osmotic pressure.

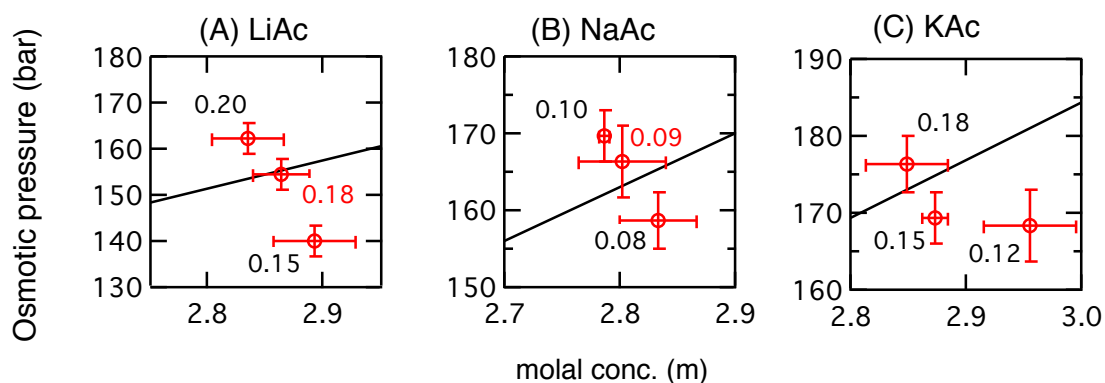


Figure S3: The effect of NBFIX correction on the osmotic pressure of Li-Ac (A), Na-Ac (B), and K-Ac (C) electrolyte solutions. All simulations reported in this figure used the standard CHARMM27 parameter set for Ac^- , Joung and Cheatham parameters for ions¹² and NBFIX correction $\Delta\sigma$ to the standard LJ σ parameter of the corresponding ion pair. Red circles plot the simulated osmotic pressure for the indicated values of the $\Delta\sigma$ correction (Å). Black lines show the experimental osmotic pressure values. Values of $\Delta\sigma$ that reproduce the experimental osmotic pressure are highlighted in red and are summarized in Table S1. For KAc (C), the value of the $\Delta\sigma$ correction was chosen to be 0.17 by interpolation.

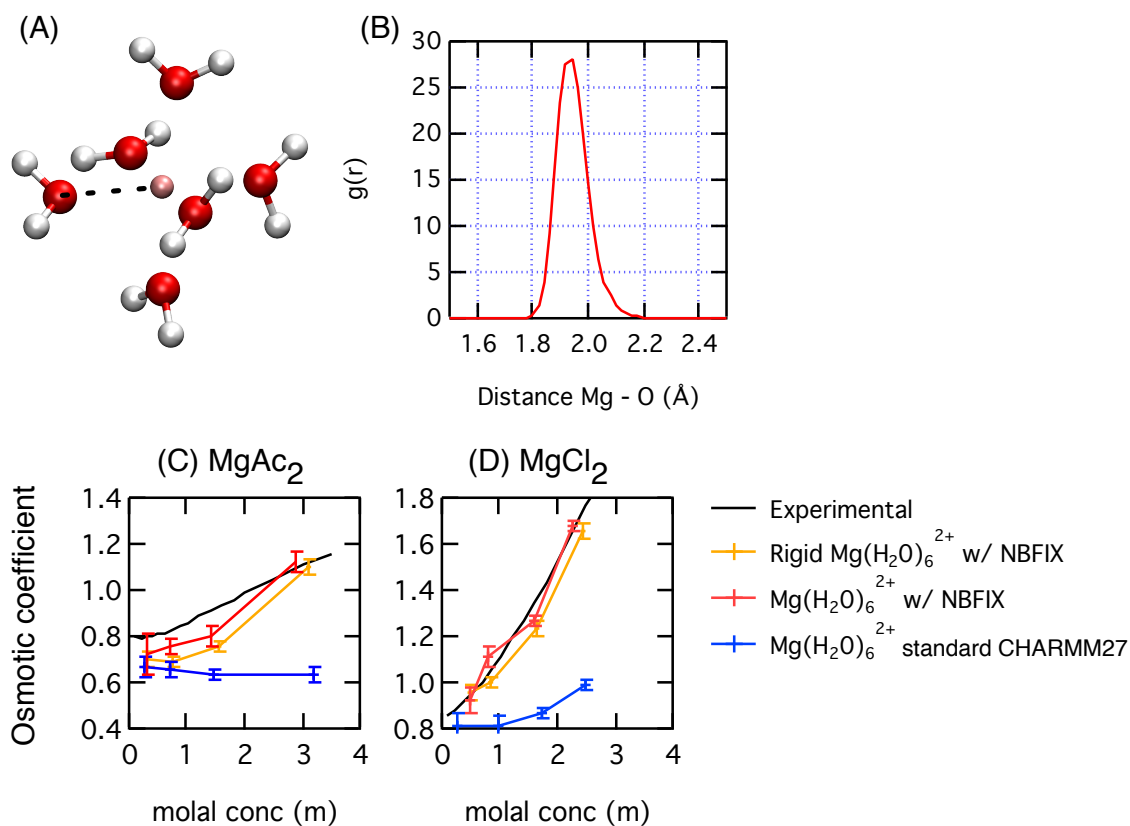


Figure S4: (A) A representative configuration of the six water molecules forming the first solvation shell of Mg^{2+} . (B) Radial distribution of water oxygen around Mg^{2+} in a $MgAc_2$ solution of ~ 0.3 m. The peak of the distribution is at 1.94 \AA . (C and D) Osmotic coefficients simulated with and without the distance constraints between Mg^{2+} and the oxygens of the first solvation shell water for $MgAc_2$ (C) and $MgCl_2$ (D) solutions. See text for details.

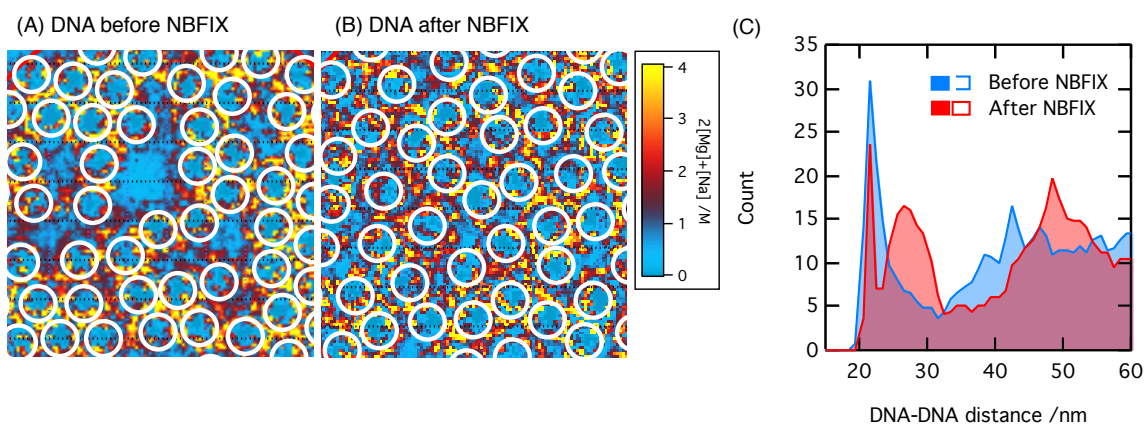


Figure S5: (A, B) Representative snapshots of the same DNA array system obtained from MD simulations performed using the standard CHARMM parameter set⁹ (A) and the standard CHARMM parameter set with our NBFIX corrections (B). Each image shows an xy cross-section of the system. The location of each DNA molecule is depicted using a white 2 nm-diameter circle. The local concentration of cations, $[\text{Na}^+] + 2[\text{Mg}^{2+}]$, averaged over the z coordinate is shown as a 2D density map. The concentration of NaCl and MgCl_2 outside the DNA array (not visible within the field of view of the image) is 250 mM and 25 mM, respectively. (C) Distribution of the DNA-DNA distances for the MD simulations depicted in panels A and B. NBFIX corrections considerably reduce the number of direct DNA-DNA contacts.

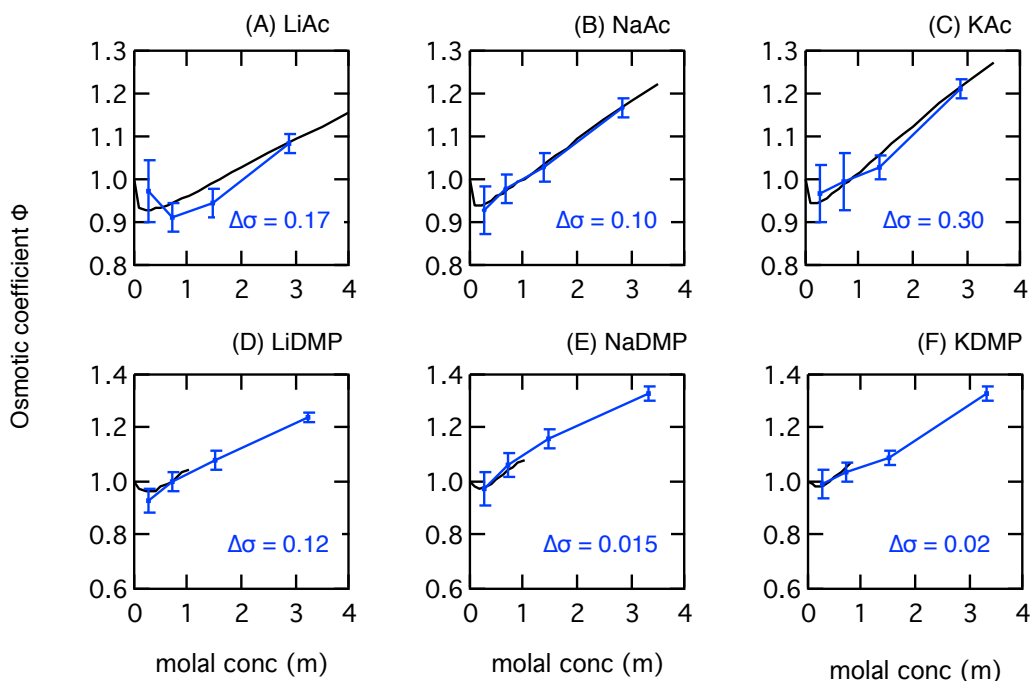


Figure S6: Simulated osmotic coefficients of Li-Ac (A), Na-Ac (B), K-AC (C), Li-DMP (D), Na-DMP (E), and K-DMP (F) solutions using the AMBER force field for Ac^- and DMP^- , Joung and Cheatham parameters for monovalent ions,¹² and NBFIX corrections as reported in Table 1. In all panels, the black lines depict the experimental osmotic coefficients.

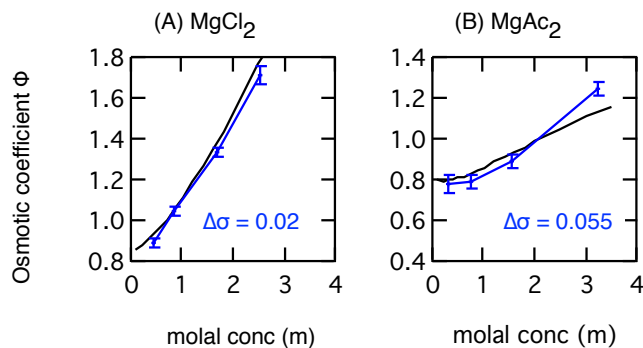


Figure S7: Simulated osmotic coefficients of MgCl_2 (A) and MgAc_2 (B) solutions using the AMBER force field for Ac^- , the CHARMM force field for Mg^{2+} , and NBFIX corrections as reported in Table 1. In all panels, the black lines depict the experimental osmotic coefficients.

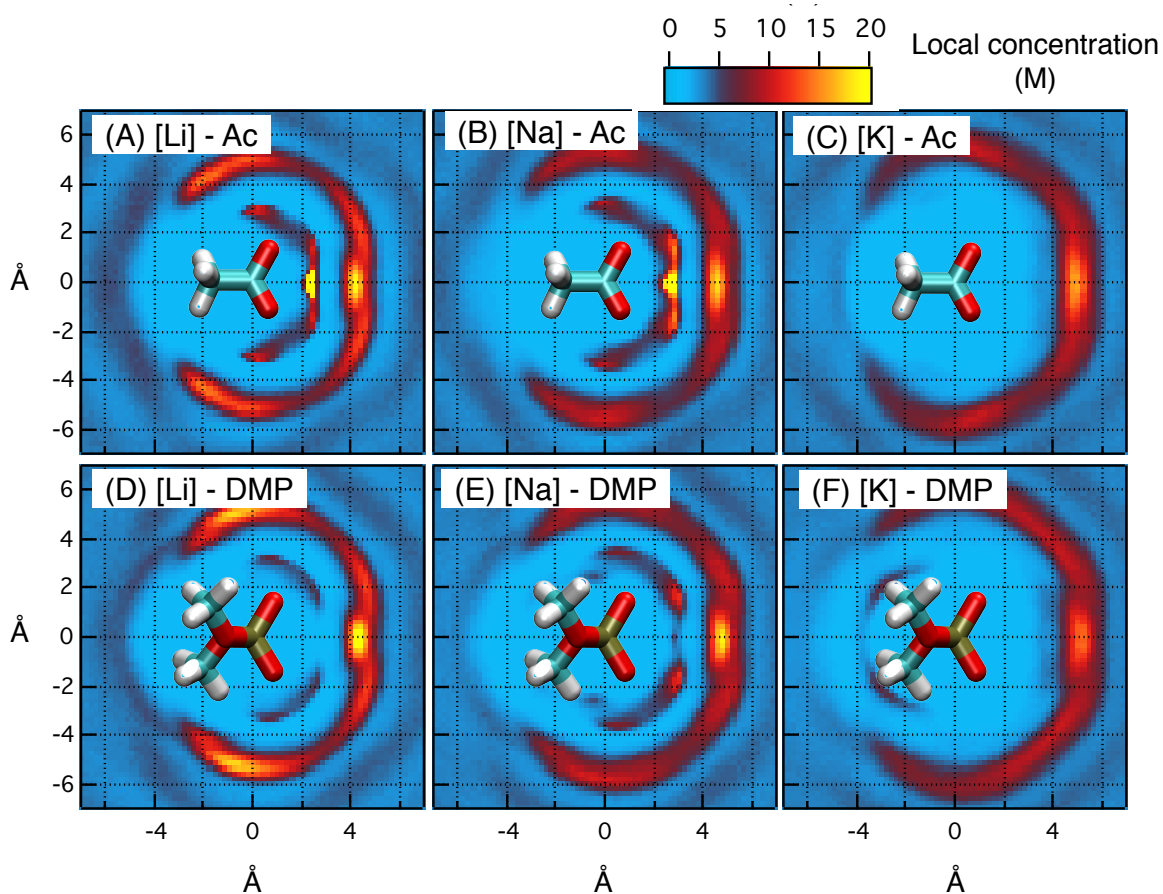


Figure S8: Local concentrations of Li^+ (A), Na^+ (B), and K^+ (C) around Ac^- and Li^+ (D), Na^+ (E), and K^+ (F) around DMP^- . All simulations reported in this figure were done using the standard AMBER force field for Ac^- and DMP^- , Joung and Cheatham parameters for monovalent ions¹² and our NBFIX correction $\Delta\sigma$ to the standard LJ σ parameter of the corresponding ion pair. The electrolyte concentration was ~ 3 m. The plane of carboxylate carbon or phosphorus and two terminal oxygens (COO or POO planes) was divided into square bins of $0.2\text{-}\text{\AA}$ width. Cations within 2 \AA from the COO or POO planes were counted.

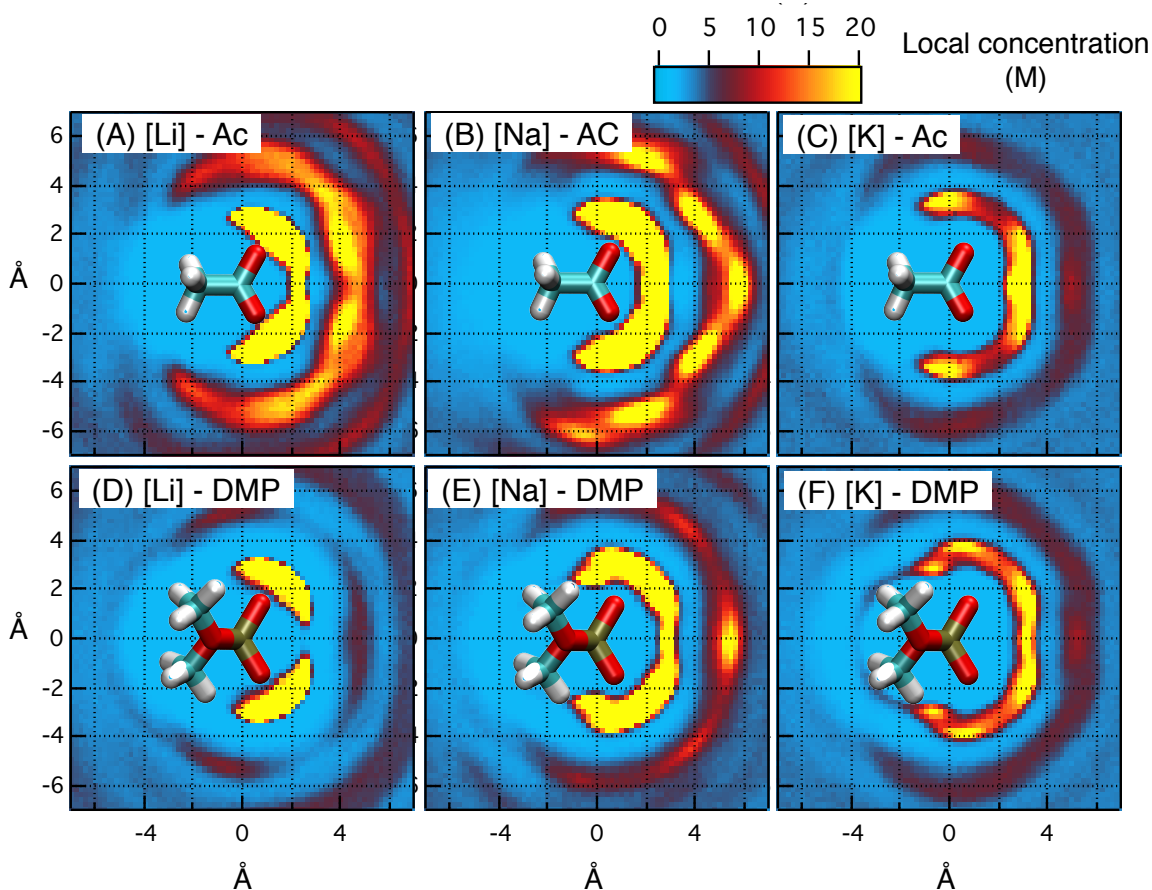


Figure S9: Local concentrations of Li^+ (A), Na^+ (B), and K^+ (C) around Ac^- and Li^+ (D), Na^+ (E), and K^+ (F) around DMP^- . All simulations reported in this figure were done using the standard AMBER force field for Ac^- and DMP^- , Joung and Cheatham parameters for monovalent ions¹² and no NBFIX corrections. The electrolyte concentration was ~ 3 m. The plane of carboxylate carbon or phosphorus and two terminal oxygens (COO or POO planes) was divided into square bins of 0.2-Å width. Cations within 2 Å from the COO or POO planes were counted.

References

- (1) Hess, B.; Kutzner, C.; Van Der Spoel, D.; Lindahl, E. GROMACS 4: Algorithms for highly efficient, load-balanced, and scalable molecular simulation. J. Chem. Theory Comput. **2008**, 4, 435–447.
- (2) Nose, S.; Klein, M. L. Constant pressure molecular dynamics for molecular systems. Mol. Phys. **1983**, 50, 1055–76.
- (3) Hoover, W. G. Canonical dynamics: Equilibrium phase-space distributions. Phys. Rev. A **1985**, 31, 1695–1697.
- (4) Tamaki, K.; Suga, K.; Tanihara, E. Solution properties of dialkyl phosphate salts - apparent molar volumes, viscosity B-coefficients, heats of solution, and osmotic coefficients. Bull. Chem. Soc. JPN **1987**, 60, 1225–9.
- (5) Parrinello, M.; Rahman, A. Polymorphic transitions in single crystals: A new molecular dynamics method. J. Appl. Phys. **1981**, 52, 7182–90.
- (6) Darden, T.; York, D.; Pedersen, L. Particle mesh Ewald: An N log(N) method for Ewald sums in large systems. J. Chem. Phys. **1993**, 98, 10089–92.
- (7) Miyamoto, S.; Kollman, P. A. SETTLE: An analytical version of the SHAKE and RATTLE algorithms for rigid water models. J. Comp. Chem. **1992**, 13, 952–62.
- (8) Hess, B.; Bekker, H.; Berendsen, H. J. C.; Fraaije, J. G. E. M. LINCS: A linear constraint solver for molecular simulations. J. Comp. Chem. **1997**, 18, 1463–72.
- (9) MacKerell Jr, A.; Banavali, N. All-atom empirical force field for nucleic acids: II. Application to molecular dynamics simulations of DNA and RNA in solution. J. Comp. Chem. **2000**, 21, 105–120.
- (10) Beglov, D.; Roux, B. Finite representation of an infinite bulk system: Solvent boundary potential for computer simulations. J. Chem. Phys. **1994**, 100, 9050–9063.

- (11) Cornell, *et.al.*, W. D. J. Am. Chem. Soc. **1995**, 117, 5179.
- (12) Joung, I. S.; Cheatham, T. E., III Determination of alkali and halide monovalent ion parameters for use in explicitly solvated biomolecular simulations. J. Phys. Chem. B **2008**, 112, 9020–9041.
- (13) Åqvist, J. Ion water interaction potentials derived from free-energy perturbation simulations. J. Phys. Chem. **1990**, 94, 8021–4.
- (14) Jorgensen, W. L.; Chandrasekhar, J.; Madura, J. D.; Impey, R. W.; Klein, M. L. Comparison of Simple Potential Functions for Simulating Liquid Water. J. Chem. Phys. **1983**, 79, 926–935.
- (15) Luo, Y.; Roux, B. Simulation of Osmotic Pressure in Concentrated Aqueous Salt Solutions. J. Phys. Chem. Lett. **2009**, 1, 183–9.
- (16) Schiferl, S.; Wallace, D. Statistical errors in molecular-dynamics averages. J. Chem. Phys. **1985**, 83, 5203–9.
- (17) McQuarrie, D. A.; Simon, J. D. Physical Chemistry: A Molecular Approach; University Science Books: Sausalito, California, 1997.
- (18) Callahan, K.; Casillas-Ituarte, N.; Roeselová, M.; Allen, H.; Tobias, D. Solvation of magnesium dication: molecular dynamics simulation and vibrational spectroscopic study of magnesium chloride in aqueous solutions. J. Phys. Chem. A **2010**, 114, 5141–8.
- (19) Jiao, D.; King, C.; Grossfield, A.; Darden, T.; Ren, P. Simulation of Ca^{2+} and Mg^{2+} solvation using polarizable atomic multipole potential. J. Phys. Chem. B **2006**, 110, 18553–9.